Mathematics Today Vol.34(A) (April 2018 – Special Issue) 76-91
ISSN 0976-3228, e-ISSN 2455-9601

Application of HAM in study of Maxwell fluid flow over stretching sheet considering effects of thermal radiation and stagnation point

Dr. Hari R. Kataria[1], Mrs. Mital H. Mistry[2]

[1]Department of Mathematics, Faculty of Science,
M. S. University of Baroda, Vadodara, India
[1]hrkrmaths@yahoo.com

[2]Department of Mathematics, Faculty of Science,
M. S. University of Baroda, Vadodara, India
[2]mhmistry29@gmail.com

Corresponding author: Mital H. Mistry[2]

Abstract

This study concerns with radiation effects on Maxwell fluid flow in presence of magnetic field. The surface is stretching and problem under consideration is two dimensional. Obtained mathematical model is system of partial differential equations. This system is transformed to system of ordinary differential equations using suitable change of variables. Expressions for velocity, heat and concentration are obtained using the homotopy analysis method. The effects of pertinent parameters are discussed graphically. The velocity increases with Stagnation point parameter but decreases with Magnetic parameter, the heat increases with Stagnation point parameter, Magnetic parameter but increases with Radiation parameter and concentration increases with Magnetic parameter, Stagnation point parameter.

Keywords: Maxwell Fluid, Thermal Radiation, Stagnation Point.
AMS Subject Classification: 76W05, 76W99**.**

Nomenclature:

a	Straining constant	Le	Lewis number
b	Constant	M	Magnetic parameter
x	Coordinate along the stretching sheet (m)	Nb	Brownian motion parameter
y	Distance normal to the stretching sheet (m)	Nt	Thermophoresis parameter
B_0	Magnetic induction (T)	s	Stagnation parameter
Bi	Biot Number	Pr	Prandtl number
C	Concentration	q_m	Mass flux (m/s)
C_∞	Ambient Concentration	q_r	Heat flux W/m^2

D_B Brownian diffusion coefficient (m^2/s)

D_T Thermophoresis diffusion coefficient (m^2/s)

f Dimensionless stream function

h Convective heat transfer coefficient (J/m^2)

k_0 Relaxation time of Maxwell fluid (s/m)

k Thermal conductivity (W/m)

U_w Stretching sheet velocity (m/s)

T Temperature of the fluid (K)

T_w Temperature at the wall (K)

T_∞ Ambient fluid temperature (K)

u, v Velocity components along x and y direction (m/s)

Greek letters:

α Thermal diffusivity

ρ Density of the fluid

ρc Heat capacity

σ Electrical conductivity

θ Dimensionless temperature

ν Kinematic viscosity

κ Maxwell fluid parameter

τ_w Wall shearing stress

η Similarity variable

ϕ Dimensionless concentration

Subscripts:

w Surface condition

∞ Condition of far away from the surface

1. Introduction

Oil and gas industries and other processes involving molten plastic, synthetic fibres, waste fluids, polymers and flows of polymer solutions are few of the applications involving non-Newtonian fluids. Thus, this attracts number of researchers, but modelling give rise to much complicated system of higher order non-linear partial differential equations.

Kataria and Mittal [1] discussed velocity, mass and temperature analysis of gravity- driven convection nanofluid flow past an oscillating vertical plate in presence of magnetic field in a porous medium. Kataria and Mittal [2] obtained mathematical model for velocity and temperature of gravity-driven convective optically thick nanofluid flow past an oscillating vertical plate in presence of magnetic field and radiation, they found that the velocity of the nanofluid increases with radiation parameter, Grashof number and time while decreases with increase in magnetic field and Prandtl number. Temperature of Nano-fluids increases with time while decrease with increase in radiation parameter and Prandtl number. Kataria and Mittal [3] investigated effect of radiation on Casson nanofluid flow. Kataria et al. [4] discussed effect of magnetic field on unsteady natural convective flow of a micropolar fluid between two vertical walls. Kataria and Patel [5] found radiation and chemical reaction effects on MHD Casson fluid flow past an oscillating vertical plate embedded in porous medium. Kataria and Patel [6] carried out soret and heat generation effects on MHD Casson fluid flow past an oscillating vertical plate embedded through porous medium. Kataria and Patel [7] investigated effects of thermo-diffusion

and parabolic motion on MHD Second grade fluid flow with ramped wall temperature and ramped surface concentration.

Liao, S. J. [8] carried out Homotopy analysis method for finding solution of the governing equations. Sheikholeslami and Rokni [9] carried out nanofluid two phase model analysis in existence of induced magnetic field, their results revealed that temperature gradient enhances with augment of suction parameter, but it reduces with augment of thermophoretic parameters. Nanofluid motion reduces with augment of Schmidt and Hartmann numbers but it enhances with augment of Buoyancy ratio and thermophoretic parameters. Sheikholeslami and Shehzad [10] discussed thermal radiation of ferrofluid in existence of Lorentz forces considering variable viscosity, their results demonstrate that rate of heat transfer enhances with augment of inclination angle. Sheikholeslami and Rokni [11] investigated free convection of CuO-H2O nanofluid in a curved porous enclosure using mesoscopic approach. They concluded that temperature gradient reduces with increase of Hartmann number while it increases with augment of permeability of porous media and buoyancy forces.

2. Governing equations

Consider two-dimensional incompressible steady Maxwell fluid over a stretching surface. Stagnation point is the origin. Plate is assumed to be along x axis, and is subject to forces of magnitude bx applied in opposite directions keeping origin fixed. Flow is along positive y direction. Physical sketch is given in Figure 1. Components of velocity along x and y axis are assumed to be u and v respectively. Here we assign a magnetic field normal to the stretching sheet. The governing equations for the continuity, momentum, energy and concentration can be written as follows:

$$\frac{\partial u}{\partial x}+\frac{\partial v}{\partial y}=0, \tag{1}$$

$$u\frac{\partial u}{\partial x}+v\frac{\partial v}{\partial y}=U_\infty\frac{dU_\infty}{dx}+v\frac{\partial^2 u}{\partial y^2}-\frac{\sigma B_0^2}{\rho}\left(u+k_0 v\frac{\partial u}{\partial y}\right)-k_0\left(u^2\frac{\partial^2 u}{\partial x^2}+v^2\frac{\partial^2 u}{\partial y^2}+2uv\frac{\partial^2 u}{\partial x\partial y}\right) \tag{2}$$

$$u\frac{\partial T}{\partial x}+v\frac{\partial T}{\partial y}=\alpha\left(\frac{\partial^2 T}{\partial y^2}\right)-\frac{1}{\rho c_p}\frac{\partial q_r}{\partial y}+D_B\left(\frac{\partial C}{\partial y}\frac{\partial T}{\partial y}\right)+\left(\frac{D_T}{T_\infty}\right)\left(\frac{\partial T}{\partial y}\right)^2 \tag{3}$$

$$u\frac{\partial C}{\partial x}+v\frac{\partial C}{\partial y}=\left(\frac{D_T}{T_\infty}\right)\left(\frac{\partial^2 T}{\partial y^2}\right)+D_B\left(\frac{\partial^2 C}{\partial y^2}\right) \tag{4}$$

Where $U_\infty=ax,\ a>0$ is the straining velocity of the flow and a is the straining constant, where u and v are the velocity component in the x and y directions, σ is the electrical conductivity, ρ is the density of the fluid, ν is the kinematic viscosity of the fluid, B_0 is the magnetic induction, α is the thermal diffusivity, k_0 is the relaxation time of the Maxwell fluid, T indicates the fluid temperature, C indicates the concentration, D_B is the Brownian diffusion coefficient, D_T is the thermophoresis diffusion coefficient, c is the volumetric expansion coefficient, T_∞ and C_∞ are denoted for the ambient values of T and C, when y tends towards infinity.

The boundary conditions for the above described model are:

$$u=U_w=bx,\ \ v=0,\ \ -k\frac{\partial T}{\partial y}=h(T_w-T),\ \ C=Cw \quad \text{at } y=0,$$

$$u\to U_\infty=ax,\ T\to T_\infty,\ \ C\to C_\infty, as\ y\to\infty. \tag{5}$$

Where the temperature has linear relationship with temperature gradient, T_w and Cw are the temperature of the fluid and concentration at the wall.

Heat flux is given as:

$$q_r = -\frac{4\sigma^*}{3k^*}\frac{\partial T^4}{\partial y} \tag{6}$$

The velocity components u and v are given as:

$$u = bxf'(\eta),\ v = -\sqrt{b\upsilon}f(\eta) \tag{7}$$

As per usual, the stream function ψ is defined as $u = \frac{\partial \psi}{\partial y}$ and $v = -\frac{\partial \psi}{\partial x}$ so that Eq. (1) is satisfied. We introduce the following dimensionless quantities:

$$\eta = \sqrt{\frac{b}{\upsilon}}y,\quad \theta(\eta) = \frac{T-T_\infty}{T_w-T_\infty},\quad \phi(\eta) = \frac{C-C_\infty}{C_w-C_\infty},\quad \psi = \sqrt{b\upsilon}xf(n) \tag{8}$$

Now substituting Eqs. (6) - (8) into Eqs. (2) - (4), we get the following system of non-linear ordinary differential equations:

$$f''' - \kappa(f^2f''' - 2ff'f'') + M^2\kappa ff'' + ff'' - M^2f' = f'^2 - s^2, \tag{9}$$

$$(1+Nr)\theta'' + \Pr\left(f\theta' + Nb\theta'\phi' + Nt\theta'^2\right) = 0, \tag{10}$$

$$\phi'' + LePrf\theta' + \frac{Nt}{Nb}\theta'' = 0. \tag{11}$$

where derivatives denote differentiation with respect to η and the transformed boundary conditions of the problem are:

$$f'(0) = 1,\quad f(0) = 0,\quad \theta'(0) = -Bi\left(1-\theta(0)\right),\quad \phi(0) = 1,$$
$$f'(\eta) = s,\quad \theta(\eta) = 0,\quad \phi(\eta) = 0,\ \text{as}\ \eta \to \infty. \tag{12}$$

where $M = \sqrt{\frac{\sigma B_0^2}{\rho b}}$ is the magnetic parameter, $s = \frac{a}{b}$ is the stagnation parameter, where $\kappa = k_0 b$ is the Maxwell fluid parameter, $Pr = \frac{\upsilon}{\alpha}$ is the Prandtl number, $Nr = \frac{16\sigma^* T_\infty^3}{3k^*k}$ is radiation parameter, $Nb = \frac{D_B(C_w-C_\infty)}{\upsilon}$ is the Brownian motion parameter, $Nt = \frac{D_T(T_w-T_\infty)}{\upsilon T_\infty}$ is the thermophoresis parameter, $Bi = \frac{\sqrt{vah}}{ak}$ is the Biot number and $Le = \frac{\alpha}{D_B}$ is the Lewis number.

3. Solution by Homotopy analysis Method

In homotopy analysis method there is great freedom to choose initial guess and auxiliary linear operator therefore, initial guesses $f_0(\eta),\ \theta_0(\eta),\ \phi_0(\eta)$ and linear operators L_f, L_θ, L_ϕ are taken in such a way that they satisfy the boundary conditions given in Eq. (12).

The initial guess is

$$f_0(\eta) = (1+s\eta)(1-e^{-\eta}),\quad \theta_0(\eta) = \frac{Bi}{Bi+1}e^{-\eta},\quad \phi_0(\eta) = e^{-\eta} \tag{13}$$

and the auxiliary linear operator are defined as

$$L_f = \frac{\partial^3 f}{\partial \eta^3} + \frac{\partial^2 f}{\partial \eta^2}, \qquad L_\theta = \frac{\partial^2 \theta}{\partial \eta^2} + \frac{\partial \theta}{\partial \eta}, \qquad L_\phi = \frac{\partial^2 \phi}{\partial \eta^2} + \frac{\partial \phi}{\partial \eta} \tag{14}$$

with $L_f(C_1 + C_2\,\eta + C_3 e^{-\eta}) = 0,\ L_\theta(C_4 + C_5 e^{-\eta}) = 0,\ L_\phi(C_6 + C_7 e^{-\eta}) = 0.$ (15)

where $c_1,\ c_2, \ldots, c_7$ are the arbitrary constants.

The zeroth order deformation problems are constructed as follows:

$$(1-p)L_f\left[\hat{f}(\eta;\, p) - f_0(\eta)\right] = p\hbar_f H_f N_f\left[\hat{f}(\eta;\, p)\right], \tag{16}$$

$$(1-p)L_\theta\left[\hat{\theta}(\eta;\, p) - \theta_0(\eta)\right] = p\hbar_\theta H_\theta N_\theta\left[\hat{\theta}(\eta;\, p)\right], \tag{17}$$

$$(1-p)L_\phi\left[\hat{\phi}(\eta;\, p) - \phi_0(\eta)\right] = p\hbar_\phi H_\phi N_\phi\left[\hat{\phi}(\eta;\, p)\right], \tag{18}$$

The nonlinear operator are defined as

$$N_f\left[\hat{f}(\eta;\, p)\right] = \frac{\partial^3 \hat{f}}{\partial \eta^3} - \kappa \hat{f}^2 \frac{\partial^3 \hat{f}}{\partial \eta^3} + \hat{f}\frac{\partial^2 \hat{f}}{\partial \eta^2} + M^2 \kappa \hat{f}\frac{\partial^2 \hat{f}}{\partial \eta^2} + 2\kappa \hat{f}\ \frac{\partial \hat{f}}{\partial \eta}\frac{\partial^2 \hat{f}}{\partial \eta^2} - \left(\frac{\partial \hat{f}}{\partial \eta}\right)^2 - M^2 \frac{\partial \hat{f}}{\partial \eta} + s^2, \tag{19}$$

$$N_\theta\left[\hat{\theta}(\eta;\, p)\right] = (1 + Nr)\frac{\partial^2 \hat{\theta}}{\partial \eta^2} + Pr\hat{f}\frac{\partial \hat{\theta}}{\partial \eta} + PrNb\frac{\partial \hat{\theta}}{\partial \eta}\frac{\partial \hat{\phi}}{\partial \eta} + PrNt\left(\frac{\partial \hat{\theta}}{\partial \eta}\right)^2, \tag{20}$$

$$N_\phi\left[\hat{\phi}(\eta;\, p)\right] = \frac{\partial^2 \hat{\phi}}{\partial \eta^2} + LePr\hat{f}\frac{\partial \hat{\phi}}{\partial \eta} + \frac{Nt}{Nb}\frac{\partial^2 \hat{\theta}}{\partial \eta^2}, \tag{21}$$

Subject to the boundary conditions:

$$\hat{f}(0;\, p) = 0, \quad \hat{f}'(0;\, p) = 1; \quad \hat{f}'(+\infty;\, p) = s, \tag{22}$$

$$\hat{\theta}'(0;\, p) = -Bi\left(1 - \hat{\theta}(0)\right),\ \hat{\theta}(+\infty;\, p) = 0, \tag{23}$$

$$\hat{\phi}(0;\, p) = 1, \quad \hat{\phi}(+\infty;\, p) = 0. \tag{24}$$

Where $\hat{f}(\eta;\, p)$, $\hat{\theta}(\eta;\, p)$ and $\hat{\phi}(\eta;\, p)$ are unknown functions with respect to η and p. $\hbar_f$, $\hbar_\theta$ and $\hbar_\phi$ are the non-zero auxiliary parameters and N_f, N_θ and N_ϕ are the nonlinear operators.

Also, where $p \in (0,\ 1)$ is an embedding parameter. For $p = 0$ and $p = 1$ we have

$$\hat{f}(\eta; 0) = f_0(\eta),\ \hat{f}(\eta; 1) = f(\eta), \tag{25}$$

$$\hat{\theta}(\eta; 0) = \theta_0(\eta),\ \hat{\theta}(\eta; 1) = \theta(\eta), \tag{26}$$

$$\hat{\phi}(\eta; 0) = \phi_0(\eta),\ \hat{\phi}(\eta; 1) = \phi(\eta), \tag{27}$$

In other word, when variation of p is taken from 0 to 1 then $\hat{f}(\eta;\, p)$, $\hat{\theta}(\eta;\, p)$ and $\hat{\phi}(\eta;\, p)$ vary from $f_0(\eta)$, $\theta_0(\eta)$, and $\phi_0(\eta)$ to $f(\eta), \theta(\eta)$, and $\phi(\eta)$. Taylor's series expansion of these functions yields the following:

$$\hat{f}(\eta;\, p) = f_0(\eta) + \sum_{m=1}^{\infty} f_m(\eta) p^m, \tag{28}$$

$$\hat{\theta}(\eta;\, p) = \theta_0(\eta) + \sum_{m=1}^{\infty} \theta_m(\eta) p^m, \tag{29}$$

$$\hat{\phi}(\eta;\, p) = \phi_0(\eta) + \sum_{m=1}^{\infty} \phi_m(\eta) p^m, \tag{30}$$

Where

$$f_m(\eta) = \frac{1}{m!}\left[\frac{\partial^m f(\eta; p)}{\partial p^m}\right]_{p=0}, \tag{31}$$

$$\theta_m(\eta) = \frac{1}{m!}\left[\frac{\partial^m \theta(\eta; p)}{\partial p^m}\right]_{p=0}, \tag{32}$$

$$\phi_m(\eta) = \frac{1}{m!}\left[\frac{\partial^m \phi(\eta; p)}{\partial p^m}\right]_{p=0}. \tag{33}$$

It should be noted that the convergence in the above series strongly depends upon $\hbar_f, \hbar_\theta$ and $\hbar_\phi$ and the proper functions $H_f(\eta)$, $H_\theta(\eta)$ and $H_\phi(\eta)$. Assuming that these nonzero auxiliary parameters are chosen so that Eqs.(28) - (30) converges at $p = 1$, Hence one can obtain the following:

$$f(\eta) = f_0(\eta) + \sum_{m=1}^{\infty} f_m(\eta), \tag{34}$$

$$\theta(\eta) = \theta_0(\eta) + \sum_{m=1}^{\infty} \theta_m(\eta), \tag{35}$$

$$\phi(\eta) = \phi_0(\eta) + \sum_{m=1}^{\infty} \phi_m(\eta), \tag{36}$$

The m^{th} order deformation equations can be presented in the form

$$L_f[f_m(\eta) - \chi_m f_{m-1}(\eta)] = \hbar_f H_f(\eta) R_{f,m}(\eta), \tag{37}$$

$$L_\theta[\theta_m(\eta) - \chi_m \theta_{m-1}(\eta)] = \hbar_\theta H_\theta(\eta) R_{\theta,m}(\eta), \tag{38}$$

$$L_\phi[\phi_m(\eta) - \chi_m \phi_{m-1}(\eta)] = \hbar_\phi H_\phi(\eta) R_{\phi,m}(\eta), \tag{39}$$

Subject to the boundary conditions

$$f_m(0) = f_m'(0) = f_m'(+\infty) = 0,$$

$$\theta_m'(0) = Bi\theta_m(0), \qquad \theta_m(+\infty) = 0,$$

$$\phi_m(0) = \phi_m(+\infty) = 0\,, \tag{40}$$

Where

$$R_{f,m}(\eta) = f_{m-1}''' - \boldsymbol{\kappa}\sum_{j=0}^{m-1} f_{m-1-j}\sum_{i=0}^{j} f_i f_{j-i}''' + \sum_{j=0}^{m-1} f_j f_{m-1-j}'' + M^2\boldsymbol{\kappa}\sum_{j=0}^{m-1} f_j f_{m-1-j}''$$
$$+ 2\boldsymbol{\kappa}\sum_{j=0}^{m-1} f_{m-1-j}\sum_{i=0}^{j} f_i' f_{j-i}'' - \sum_{j=0}^{m-1} f_j' f_{m-1-j}' - M^2 f_{m-1}' + s^2(1-\chi_m) \tag{41}$$

$$R_{\theta,m}(\eta) = \ (1+N_r)\theta_{m-1}'' + Pr\sum_{j=0}^{m-1} f_j\theta_{m-1-j}' + PrNb\sum_{j=0}^{m-1}\theta_j'\phi_{m-1-j}' + PrNt\sum_{j=0}^{m-1}\theta_j'\theta_{m-1-j}'\,, \tag{42}$$

$$R_{\phi,m}(\eta) = \ \phi_{m-1}'' + LePr\sum_{j=0}^{m-1} f_j\,\phi_{m-1-j}' + \frac{Nt}{Nb}\,\theta_{m-1}''. \tag{43}$$

$$\text{with } \chi_m = \begin{cases} 0, & m \le 1 \\ 1, & m \ge 1 \end{cases}, \tag{44}$$

To assure the convergence, the auxiliary functions $H_f(\eta),\ H_\theta(\eta),\ H_\phi(\eta)$ are selected as

$$H_f(\eta) = H_\theta(\eta) = H_\phi(\eta) = e^{-\eta}. \tag{45}$$

The general solutions $f_m, \theta_m \ and\ \phi_m$ comprising the special solution $f_m^*, \theta_m^* \ and\ \phi_m^*$ are given by

$$f_m(\eta) = f_m^*(\eta) + C_1 + C_2\,\eta + C_3 e^{-\eta}, \tag{46}$$

$$\theta_m(\eta) = \theta_m^*(\eta) + C_4 + C_5 e^{-\eta}, \tag{47}$$

$$\phi_m(\eta) = \phi_m^*(\eta) + C_6 + C_7 e^{-\eta}. \tag{48}$$

Here $f_m^*, \theta_m^* \ and\ \phi_m^*$ are given by are particular solutions of the corresponding mth-order equations and the constants $C_i(\ i = 1,2,\dots,7)$ are to be determined by the boundary conditions.

5. Convergence of the series solutions:

Convergence of the HAM solutions and their rate of approximations strongly depend on the values of the auxiliary parameters $\hbar_f, \hbar_\theta$ and $\hbar_\phi$. For this purpose, the associated h-curve is plotted in Figure 2. In the present case, H-curve of $f''(0)$ is plotted taking appropriate order. The Figure 2 clearly suggest admissible range $-0.7 \le \hbar_f \le -0.1$ for the auxiliary parameter $\hbar_f$. Here we take $\hbar_f = -0.6$, Similarly we take values for $\hbar_\theta = -0.8$ and $\hbar_\phi = -0.4$.

6. Result:

In this section, to acquire a rich understanding on the physics of the problem, the solutions are obtained using appropriate codes in Mathematica. Obtained results are explained with the help of graphs. Through Figures 3 - 13, the contribution of various parameter like the Magnetic parameter M, the Maxwell fluid parameter κ, the Stagnation parameter S, the Lewis number Le, the Prandtl number Pr, the Biot number Bi, the Thermophoresis parameter N_t and the Brownian parameter N_b on the velocity, the temperature and the concentration distributions are discussed in detail.

Influence of the Maxwell fluid parameter κ on the velocity profile is displayed in Figure 3. It can be noticed that the velocity of the fluid decreases with increasing Maxwell fluid parameter κ.

Figure 4 describes that the velocity decreases as M increases. The increased Magnetic parameter, means enhanced Lorentz force, which resists the flow. Figure 5 shows that an increase in the stagnation parameter s creates widening in the velocity profile. Figure 6 depicts behavior of the Maxwell fluid parameter κ on temperature profile. It can be noticed that temperature profile increases as the Maxwell fluid parameter increases.

Effect of Magnetic parameter M on the temperature profile in shown in Figure 7. The presence of stronger Magnetic field increases the temperature profile. Figure 8 illustrates the variation in temperature profile for different values of the stagnation parameter s. we can notice that as stagnation parameter rises, temperature profile increases. Figure 9 depicts that temperature increases with increase in radiation parameter Nr. It is clear from Figure 10 that as the Maxwell fluid parameter κ increases the concentration rises.

In Figure 11, It can be observed that concentration increases for large value of magnetic parameter M. It is noticeable in Figure 12 that as stagnation parameter increases the concentration increases. Effect of Radiation Parameter Nr on concentration profile is depicted in Figure 13. It can be observed that concentration profile increases as radiation parameter increases.

7. Conclusion:

- Fluid velocity declines with Maxwell fluid parameter κ and magnetic parameter M.
- Fluid velocity increases with stagnation parameter s.
- Fluid temperature can be increased by increasing either of Maxwell fluid parameter κ, Magnetic parameter M, Radiation parameter *Nr* or stagnation parameter s.
- Fluid Concentration can be increased by increasing either of Maxwell Fluid parameter, Magnetic parameter, stagnation parameter or Radiation parameter *Nr*.

References:

[1] Kataria, H. R. and Mittal, A., (2015): Mathematical model for velocity and temperature of gravity-driven convective optically thick nanofluid flow past an oscillating vertical plate in presence of magnetic field and radiation. Journal of Nigerian Mathematical Society, 34, 303–317.

[2] Kataria, H. R. and Mittal, A. S., (2017): Velocity, mass and temperature analysis of gravity-driven convection nanofluid flow past an oscillating vertical plate in presence of magnetic field in a porous medium, Applied Thermal Engineering, 110, 864-874.

[3] Kataria, H. R., Mittal, A. S., (2017): Analysis of Casson nanofluid flow in presence of magnetic field and radiation, Mathematics Today, 33(1), 99 - 120.

[4] Kataria, H. R., Patel, H. R. and Singh, R., (2015): Effect of magnetic field on unsteady natural convective flow of a micropolar fluid between two vertical walls. Ain Shams Engineering Journal, doi. 10.1016/j.asej.2015.08.013.

[5] Kataria, H. R. and Patel, H. R., (2016): Radiation and chemical reaction effects on MHD Casson fluid flow past an oscillating vertical plate embedded in porous medium, Alexandria Engineering Journal, 55, 583-595.

[6] Kataria, H. R. and Patel, H. R., (2016): Soret and heat generation effects on MHD Casson fluid flow past an oscillating vertical plate embedded through porous medium, Alexandria Engineering Journal 55, 2125–2137.

[7] Kataria, H. R. and Patel, H. R., (2016): Effect of thermo-diffusion and parabolic motion on MHD Second grade fluid flow with ramped wall temperature and ramped surface concentration, Alexandria Engineering Journal, 10.1016/j.aej.2016.11.014.

[8] Liao, S. J., (2003): Beyond perturbation: Introduction to homotopy Analysis Method, Chapman and Hall/CRC Press, Boca Raton.

[9] Sheikholeslami, M. and Rokni, H. B., (2017):Nanofluid two phase model analysis in existence of induced magnetic field, International Journal of Heat and Mass Transfer 107 (2017) 288–299.

[10] Sheikholeslami, M. and Shehzad, S.A., (2017): Thermal radiation of ferrofluid in existence of Lorentz forces considering variable viscosity, International Journal of Heat and Mass Transfer 109 (2017) 82–92.

[11] Sheikholeslami and M., Rokni, H. B., (2017): Free convection of CuO-H2O nanofluid in a curved porous enclosure using mesoscopic approach, International Journal of Hydrogen Energy, 42(2017), 14942-14949.

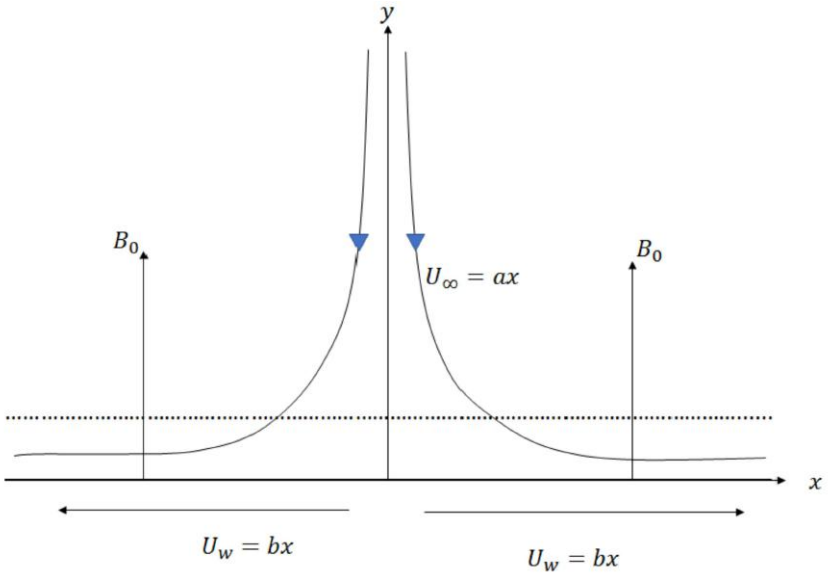

Fig 1: Physical sketch of the problem.

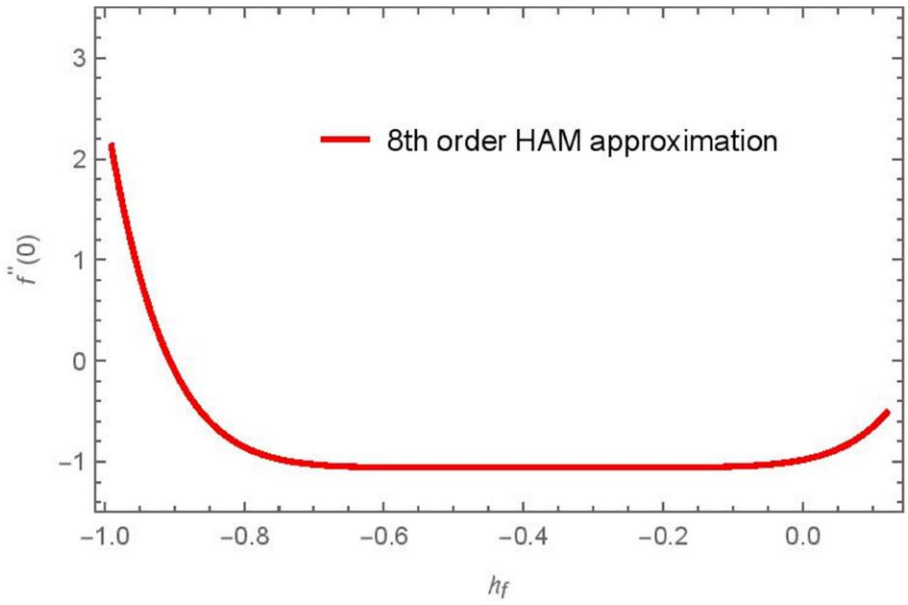

Fig 2: The H-Curve of $f''(0)$ for different values of $\hbar_f$ for 8th HAM approximation at M = 1.2, Pr = 6.7, s = 0.01, Bi =0.1, Nb = 0.2, Nt = 0.2, Le = 0.5, κ = 0.05, $Nr = 2.0$

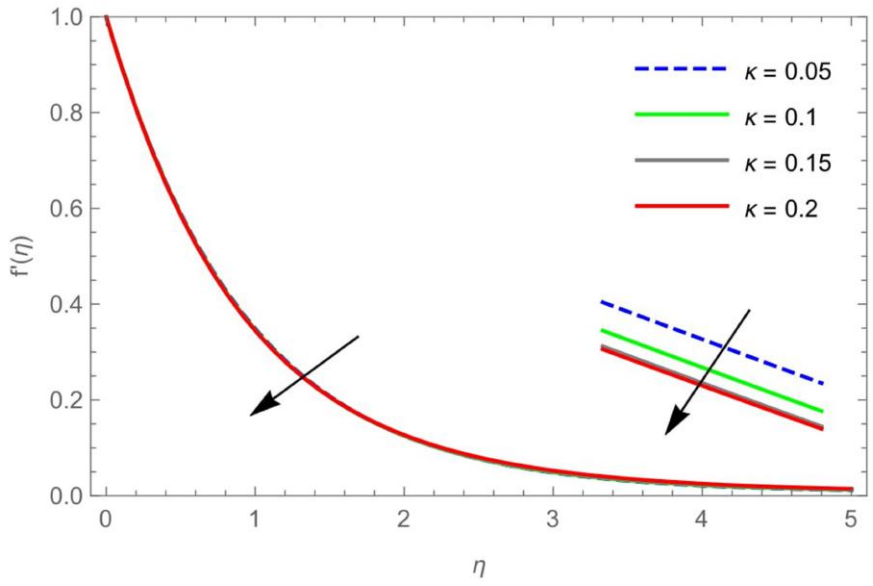

Fig 3: Velocity profile f' for different values of η and κ at $\mathbf{M = 1.2,\ s = 0.01,\ Pr = 6.7,\ Nb = 0.2,\ Nr = 2.0,\ N\,t = 0.2,\ Le = 0.5,\ Bi = 1.0}$

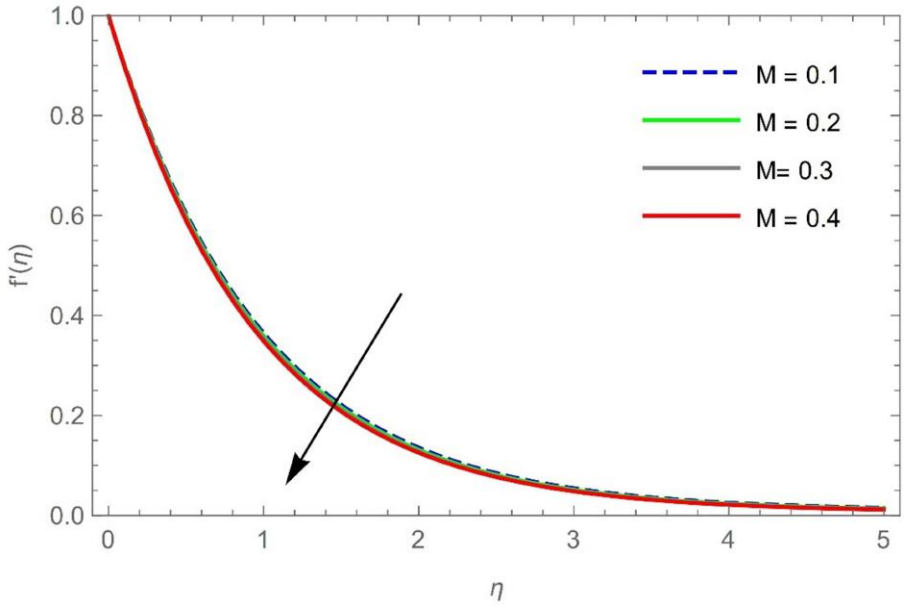

Fig 4: Velocity profile f' for different values of η and M at $\kappa = 0.05,\ Bi = 0.1,\ s = 0.01,\ Pr = 6.7,\ Nb = 0.2,\ Nt = 0.2,\ Le = 0.5,\ Nr = 2.0$

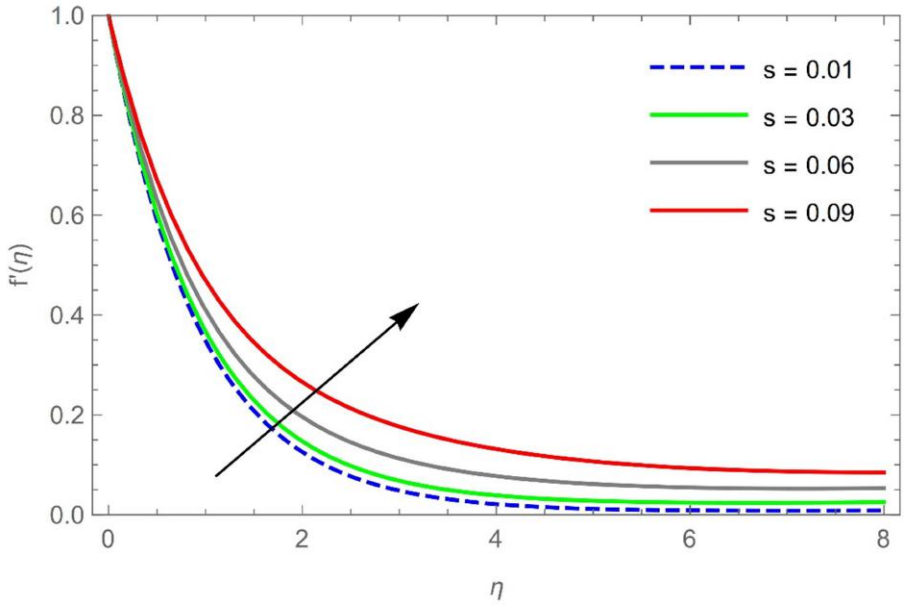

Fig 5: Velocity profile u for different values of η and s at $\mathbf{M = 0.4,\ Le = 0.5,\ Pr = 6.7,\ Nb = 0.2,\ Nt = 0.2,\ Bi = 0.1,\ \kappa = 0.05,\ Nr = 2.0}$

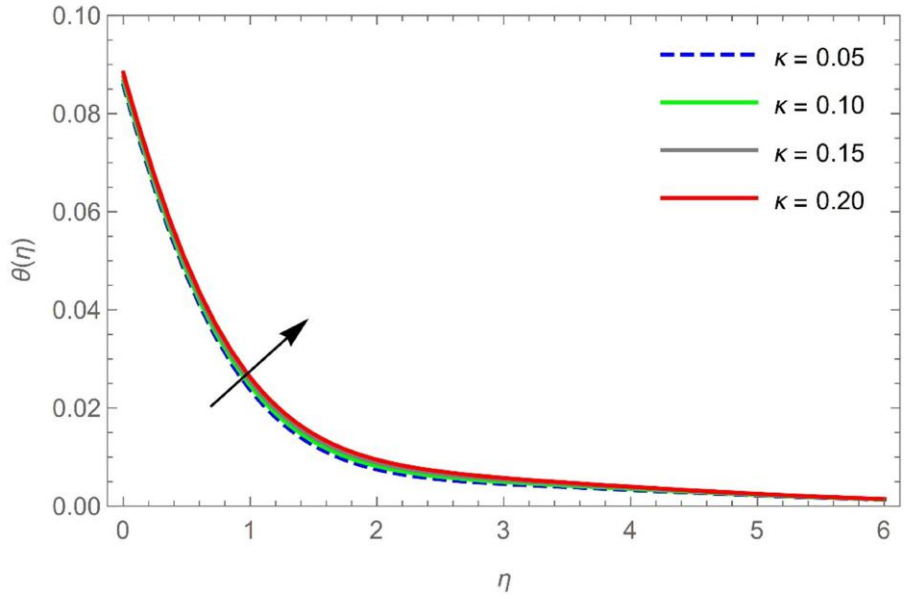

Fig 6: Temperature profile θ for different values of η and κ at $\mathbf{M = 1.2,\ Bi = 0.1,\ s = 0.01,\ Nt = 0.2,\ Nb = 0.2,\ Le = 0.5, Pr = 6.7, Nr = 2}$

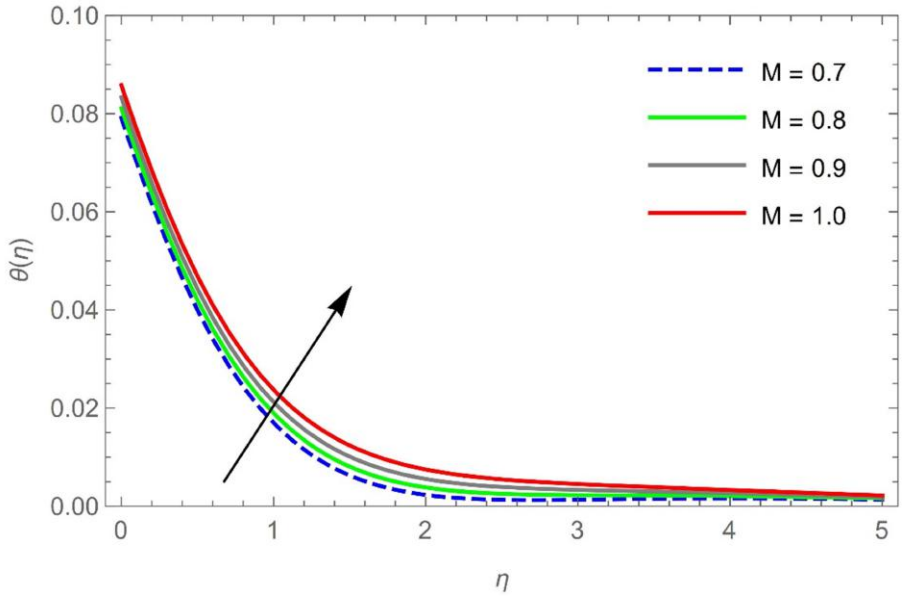

Fig 7: Temperature profile θ for different values of η and M at $\mathbf{Le} = 0.5$, $\mathbf{Bi} = 0.1$, $\mathbf{s} = 0.01$, $\mathbf{Nt} = 0.2$, $\mathbf{Nb} = 0.2$, $\kappa = 0.05$, $Pr = 6.7$, $\mathbf{Nr} = 2.0$

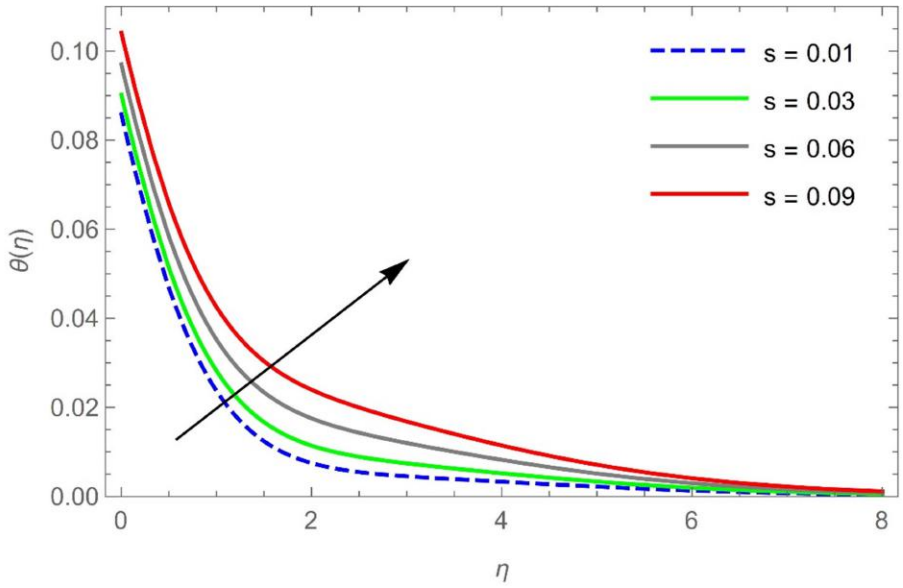

Fig 8: Temperature profile θ for different values of η and s at $\mathbf{M} = 1.2$, $\mathbf{Bi} = 0.1$, $\mathbf{Nb} = 0.2$, $\mathbf{Nt} = 0.2$, $\mathbf{Le} = 0.5$, $\kappa = 0.05$, $Pr = 6.7$, $\mathbf{Nr} = 2.0$

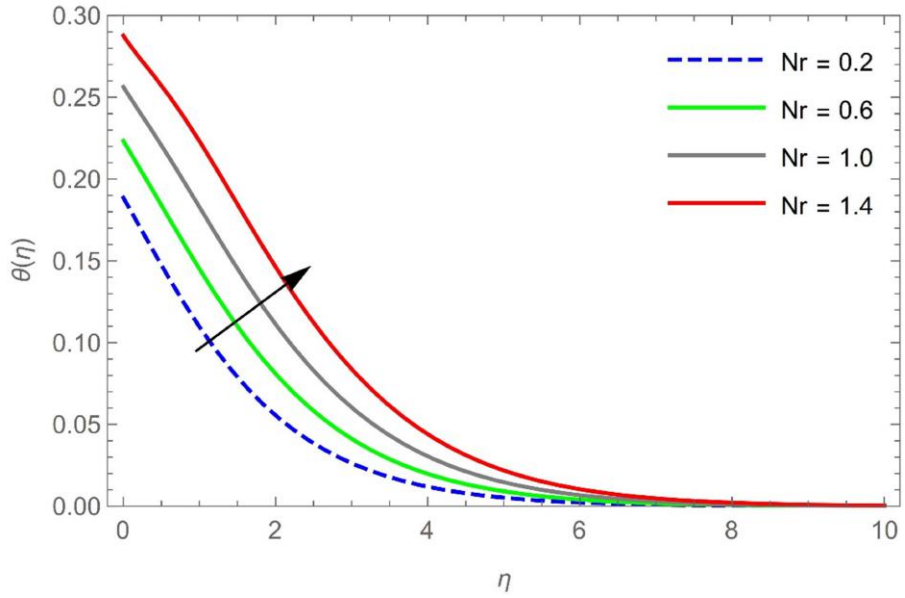

Fig 9: Temperature profile θ for different values of η and Nr at $\mathbf{M = 1.2,\ Bi = 0.1,\ Nb = 0.2,\ Nt = 0.2,\ Le = 0.5,\ \kappa = 0.05,\ Pr = 6.7,\ s = 0.01}$

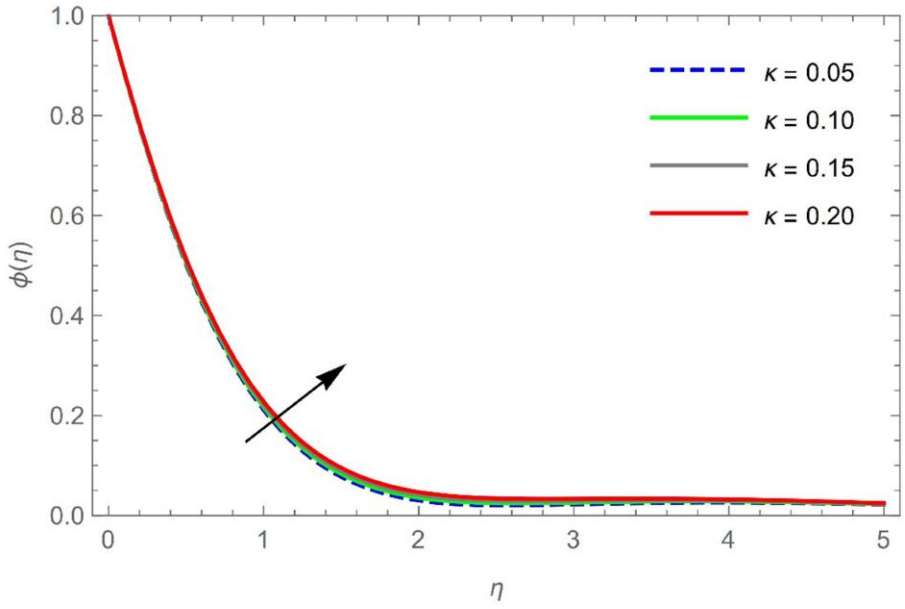

Fig 10: Concentration profile ϕ for different values of η and κ at $\mathbf{M = 1.2,\ Bi = 0.1,\ Nb = 0.2,\ Nt = 0.2,\ Le = 0.5,\ Pr = 6.7,\ s = 0.01,\ Nr = 2.0}$

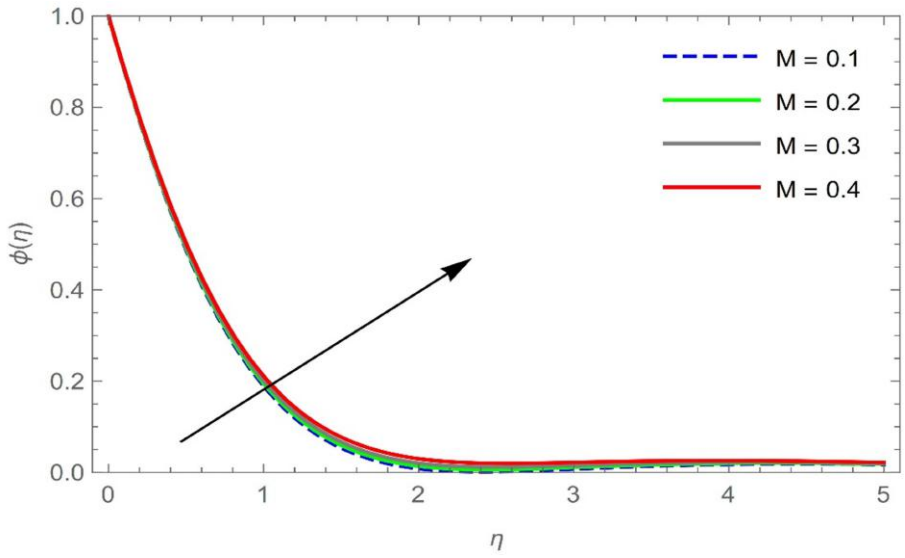

Fig 11: Concentration profile ϕ for different values of η and M at Le $= 0.5$, Bi $= 0.1$, Nb $= 0.2$, Nt $= 0.2$, $\kappa = 0.05$, $Pr = 6.7$, $s = 0.01$, Nr $= 2.0$

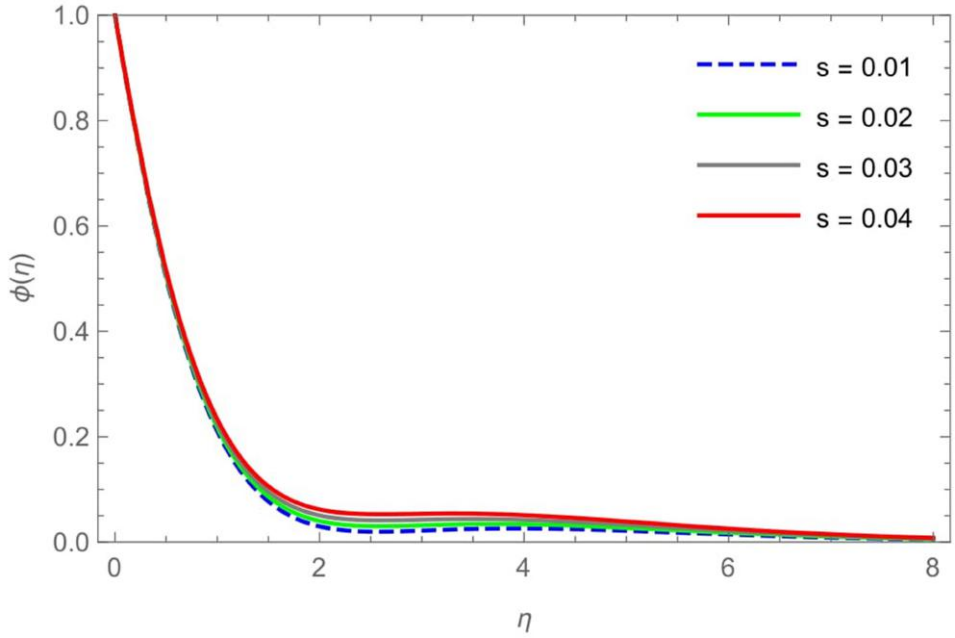

Fig 12: Concentration profile ϕ for different values of η and s at Le $= 0.5$, Bi $= 0.1$, Nb $= 0.2$, Nt $= 0.2$, $\kappa = 0.05$, $Pr = 6.7$, $M = 1.2$, Nr $= 2.0$

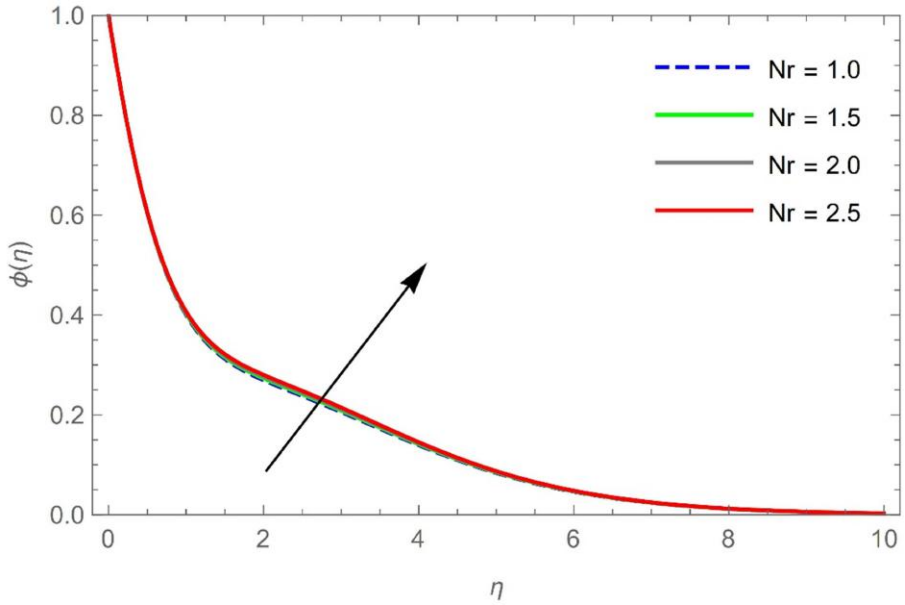

Fig 13: Concentration profile ϕ for different values of η and Nr at $\mathbf{Le} = 0.5$, $\mathbf{Bi} = 0.1$, $\mathbf{Nb} = 0.2$, $\mathbf{Nt} = 0.2$, $\kappa = 0.05$, $Pr = 6.7$, $s = 0.01$, $\mathbf{M} = 1.2$